

## ORIGINAL RESEARCH ARTICLE

# Numerical analysis of the flow parameters on the heat transfer performance of a two-stage spiral casing heat exchanger

Zhiqiang Li<sup>1,2</sup>, Xianfei Liu<sup>1,2</sup>, Fang Wang<sup>1,2\*</sup>, Caixia Zhu<sup>1,2</sup>, Haofei Zhang<sup>1,2</sup>, Shiyuan Wang<sup>1,2</sup>

<sup>1</sup> School of Energy and Environment, Zhongyuan University of Technology, Zhengzhou 450007, Henan province, China.  
E-mail: fwang@zut.edu.cn.

<sup>2</sup> Research Center of LNG Cold Energy Utilization Engineering of Henan Province, Zhengzhou 450007, Henan province, China.

## ABSTRACT

The study of the performance of high-efficiency heat pump systems has been a hot issue of general interest in the field of heat pump air conditioning. For the designed and developed two-stage casing tandem heat exchanger of heat pump system, the 3D finite volume method and the realizable k- $\epsilon$  model are used to numerically analyze the influence law of inlet fluid temperature and flow velocity on the overall heat transfer coefficient as well as the Nusselt number of inner and outer tubes. The results show that decreasing the inlet water temperature or increasing the inlet refrigerant temperature can improve the overall heat transfer performance;  $Nu_{in}$  increases with the increase of water and refrigerant flow rates, while  $Nu_{out}$  increases with the increase of water flow rate but decreases with the increase of refrigerant flow rate;  $Nu_{in}$  and  $Nu_{out}$  both increase with the decrease of water temperature or refrigerant temperature increases.

**Keywords:** Flow Parameter; Heat Pump; Spiral Tube Heat Exchanger; Heat Transfer Performance; Nusselt Number

## ARTICLE INFO

Received: 27 January 2022  
Accepted: 3 March 2022  
Available online: 13 March 2022

## COPYRIGHT

Copyright © 2022 Zhiqiang Li, *et al.*  
EnPress Publisher LLC. This work is licensed under the Creative Commons Attribution-NonCommercial 4.0 International License (CC BY-NC 4.0).  
<https://creativecommons.org/licenses/by-nc/4.0/>

## 1. Introduction

As one of the main components of a heat pump system, the cased heat exchanger directly determines the performance of the heat pump air conditioning system. With the increasing demand for developing and improving the efficiency of heat exchangers, it is important to improve the heat transfer efficiency of heat exchangers, which has a guiding impact on the cycle performance of heat pump air conditioning systems<sup>[1]</sup>. Researchers have conducted a lot of theoretical analyses and experimental studies on the simulation modeling, optimization of design parameters and practical applications of casing-type heat exchangers, which have contributed to the improvement of the overall performance of casing-type heat exchangers<sup>[2,3]</sup>.

Ren *et al.*<sup>[4]</sup> optimized the design of multi-casing heat exchanger and compared the analysis of single-casing heat exchanger, the heat transfer coefficient of multi-casing casing type heat exchanger has been greatly improved. Liao<sup>[5]</sup> used CFX simulation software to analyze the fluid velocity and temperature distribution of cased heat exchangers with different internal diameters and compared the heat transfer coefficients under different operating conditions, pointing out that the heat transfer effect of casing increases gradually with the increase of eccentricity. Zhang *et al.*<sup>[6]</sup> conducted an experimental study on the heat transfer characteristics of mixed mass R417a in a spiral casing heat ex-

changer under different operating conditions, pointing out that the heat transfer coefficient decreases continuously with the increase of condensation temperature, and the local condensation heat transfer coefficient shows an increasing pattern with the increase of dryness. Lv *et al.*<sup>[7]</sup> investigated the effect of different CO<sub>2</sub> mass flow rates, inlet pressure and cooling water temperature on the flow heat transfer characteristics of a triple casing gas cooler, and the results showed that the heat transfer coefficient and the heat exchange rate showed a trend of increasing and then decreasing with the increase of mass flow rate. Ma *et al.*<sup>[8]</sup> studied the variation of heat transfer coefficient of evaporative condensation in terms of heat flow density, air volume and water flow, and gave the minimum air and water volume distribution. Chen and Gan<sup>[9]</sup> dynamically evaluated the heat exchanger performance of the casing heat exchanger at different high temperature fluid temperatures to study the temperature variation distribution law.

Colorado-Garrido *et al.*<sup>[10]</sup> studied the fluid characteristics and heat transfer performance of a vertical spiral casing evaporator, where the intra-tube pressure and annular temperature were the two important parameters determining the outlet temperature increase. Wu *et al.*<sup>[11]</sup> conducted an experimental study of pressure drop and heat transfer in a spiral tube heat exchanger using nanofluid, which was not significantly enhanced by the nanofluid. Elattar *et al.*<sup>[12]</sup>, Fouda *et al.*<sup>[13]</sup> studied the heat transfer performance of a multi-tube spiral tube heat exchanger under turbulent flow conditions and analyzed the effect of flow parameters and structural parameters on the thermal, hydrodynamic characteristics of the spiral tube heat exchanger. The comparison between the multi-tube spiral tube heat exchanger and the straight tube heat exchanger shows that the multi-tube spiral tube heat exchanger has better thermal performance and the maximum value of the combined thermo-hydraulic performance factor occurs at  $N = 3$ .

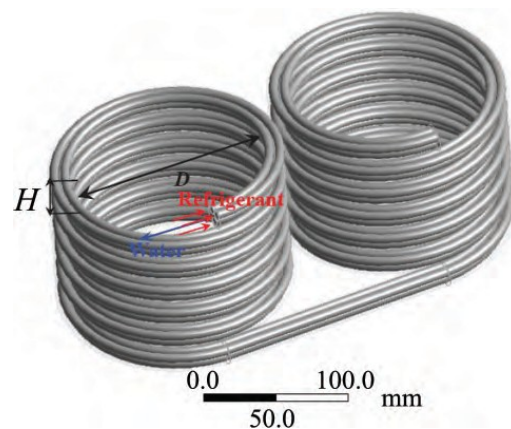
There are few studies on the flow heat transfer characteristics of the two-stage spiral casing heat exchanger connected by straight pipe sections. The effect of structural parameters on the flow heat

transfer performance of heat exchangers, the effect of structural parameters and inner and outer tube flow rates on the overall heat transfer coefficients,  $\epsilon$ -NTU, pump work and pressure drop, combined thermohydraulic performance factors and inner and outer tube Nusselt number were previously discussed by this group<sup>[14]</sup>, and the preliminary experimental studies showed that this structure heat exchanger has better heat transfer efficiency<sup>[15,16]</sup>. This study aims to further reveal the influence of flow parameters on the heat transfer performance of a two-stage spiral casing heat exchanger, and the results will provide theoretical guidance for efficient heat exchanger operation in heat pump systems.

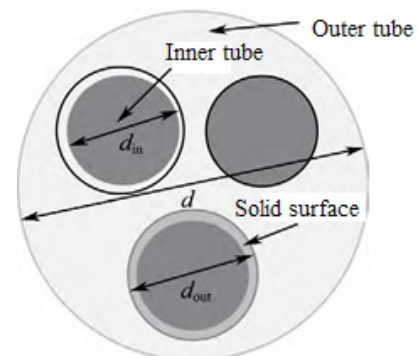
## 2. Numerical model

### 2.1 Physical model

The physical model of a two-stage spiral casing heat exchanger and its internal and external tube structure characteristics are given in **Figure 1**.



(a) Physical model of the two-stage spiral casing heat exchanger



(b) Structural characteristics of the inner and outer tubes  
**Figure 1.** 3D structure parameter schematic of two-stage helically coiled heat exchangers.

The tests were conducted under counter-flow conditions, where cold water flowed in the annular region of the casing with an inlet temperature of 299.0 K and HFC125 refrigerant flowed in the internal tube with an inlet temperature of 259.3 K. The number of internal tubes of the casing heat exchanger was three and symmetrically distributed. The spiral casing structure parameters considered in this study were a spiral diameter length of  $D = 150.0$  mm and a spiral pitch of  $H = 22.5$  mm, where the inner tube inner diameter was taken as  $d_{in} = 6.0$  mm, the inner tube outer diameter as  $d_{in} = 7.0$  mm, and the outer tube diameter as  $d = 19.0$  mm<sup>[14]</sup>.

## 2.2 Numerical methods

The 3D control equations for turbulence and heat transfer in a heat exchanger can be written in tensor form in the Cartesian principal system, for numerical simulations, it is necessary to consider the assumptions:

- i. The flow is considered to be stable, incompressible.
- ii. The inlet flow is used as the overall mass flow.
- iii. The physical parameters of flow and heat transfer are considered to be constant.

Continuity equation:

$$\frac{\partial u_i}{\partial x_i} = 0 \quad (1)$$

Conservation of momentum equation:

$$\rho u_i \frac{\partial (u_i)}{\partial x_i} = -\frac{\partial p}{\partial x_j} + \frac{\partial}{\partial x_i} \left( \mu \left( \frac{\partial u_i}{\partial x_i} + \frac{\partial u_j}{\partial x_i} \right) - \overline{\rho u_i' u_j'} \right) \quad (2)$$

Energy equation:

$$\rho u_i \frac{\partial (T)}{\partial x_i} = \frac{\partial}{\partial x_j} \left( \lambda \left( \frac{\partial T}{\partial x_i} - \rho c_{p\rho} \overline{u_i' T_j'} \right) \right) \quad (3)$$

The boundary conditions are set as velocity inlet boundary for the inlet and pressure let boundary for the outlet. For the heat fer between the inner and outer tubes of the heat exchanger, the thermal conductivity of the solid walls is also considered and the adiabatic conditions are used for the exterior of the heat exchanger.

## 2.3 Numerical calculations

The numerical simulation software used in this paper is FLUENT 15.0, and the achievable  $k-\varepsilon$  turbulence model is used to predict the flow and heat transfer because it can accurately predict the bending and vortex flow compared to other  $k-\varepsilon$  turbulence models, and also has superior performance in terms of computational time<sup>[13]</sup>. The velocity, pressure and temperature variables are calculated by the finite volume method, and the coupled velocity and pressure problem is solved by the PISO algorithm, with the pressure equations discretized in second-order format and the momentum and energy equations discretized in second-order windward format, with the residuals of continuity and energy  $10^{-7}$  and  $10^{-9}$ . The computational domain is divided with uniform grids, and to ensure the accuracy of the solution and save computational time, the computational domain is first meshed with six mesh scales of  $0.599 \times 10^6$ ,  $0.652 \times 10^6$ ,  $0.891 \times 10^6$ ,  $1.307 \times 10^6$ ,  $1.645 \times 10^6$  and  $1.89 \times 10^6$  for verification, and the results are shown in **Figure 2**. And compared with the  $1.897 \times 10^6$  grid calculation results, the relative error of the  $1.645 \times 10^6$  calculation results was less than 0.015%, and the second model results were verified with the preliminary experimental results<sup>[14]</sup>. The numerical model of this paper can be used to evaluate the flow and heat transfer characteristics of spiral casing heat exchanger.

## 2.4 Data processing

The overall heat transfer coefficient was calculated from the heat transfer and the external area of the inner tube, and the heat transfer was defined as the average value between the heat released by HFC125 and the heat absorbed by the cooling water<sup>[12,13]</sup>.

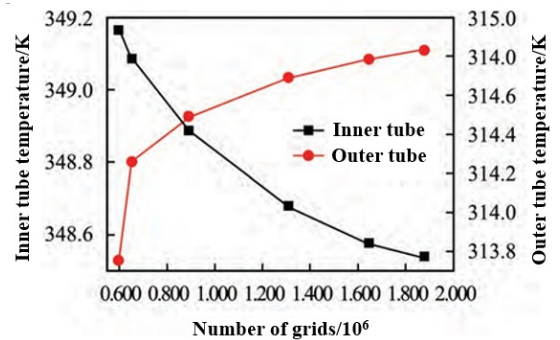


**Figure 2.** Outlet temperature of the calculated domain under different grids.

$$h = \frac{\Phi_{\text{avg}}}{A_{\text{out}} \Delta T_{\text{LMTD}}} \quad (4)$$

$$\Phi_{\text{avg}} = \frac{\Phi_w + \Phi_{\text{ref}}}{2} \quad (5)$$

$$\Delta T_{\text{LMTD}} = \frac{\Delta T_{\text{max}} - \Delta T_{\text{min}}}{\ln\left(\frac{\Delta T_{\text{max}}}{\Delta T_{\text{min}}}\right)} \quad (6)$$

Average heat transfer coefficient and Nussle number are calculated as:

$$h_{\text{ref}} = \frac{\Phi_{\text{avg}}}{A_{\text{in}} (T_{\text{ref, avg}} - T_{\text{si, avg}})} \quad (7)$$

$$h_w = \frac{\Phi_{\text{avg}}}{A_{\text{out}} (T_{\text{si, avg}} - T_{\text{w, avg}})} \quad (8)$$

$$Nu_{\text{ref}} = \frac{h_{\text{ref}} d_{\text{in}}}{k_{\text{ref}}} \quad (9)$$

$$Nu_w = \frac{h_w d_c}{k_w} \quad (10)$$

In the equation:  $d_c$  is the equivalent diameter of the outer tube,  $T_{\text{si, avg}}$  is the average solid interface temperature,  $T_{\text{ref, avg}}$  and  $T_{\text{w, avg}}$  are the average temperatures of the refrigerant and cold water, respectively.

### 3. Results and Discussion

#### 3.1 Effect of inlet water temperature on flow and heat transfer performance

Figures 3(a) and (b) gives the variation of the overall heat transfer coefficient with flow rate for different inlet water temperatures. The results show that the overall heat transfer coefficient increases by 19.27% with the increase in the flow rate of the outer tube water for a constant flow rate of the inner tube refrigerant, which is attributed to the increase in the heat transfer rate and the decrease in the average temperature difference due to the increase in the flow rate of the cold water, which is consistent with the variation of the overall heat transfer coefficient of the multi-tube spiral heat exchanger in the

literature<sup>[13]</sup>. Under the constant flow rate of water, increasing the flow rate of the inner tube refrigerant leads to a significant increase in the temperature difference, resulting in a decrease in the overall heat transfer coefficient by 15.69% with the increase in refrigerant flow rate, although there is an increase in the overall heat transfer<sup>[17]</sup>, which is due to the higher flow rate and higher temperature of the inner tube refrigerant compared to water, increasing the refrigerant flow. This indicates that the inner tube refrigerant flow rate is the limiting factor for the increase of the overall heat transfer coefficient in this operating range. It is also found that the overall heat transfer coefficient increases with the decrease of inlet water temperature, which is a significant increase in heat transfer due to lower inlet water temperature and a decrease in temperature difference, resulting in an increase of 6.82% in the overall heat transfer coefficient.

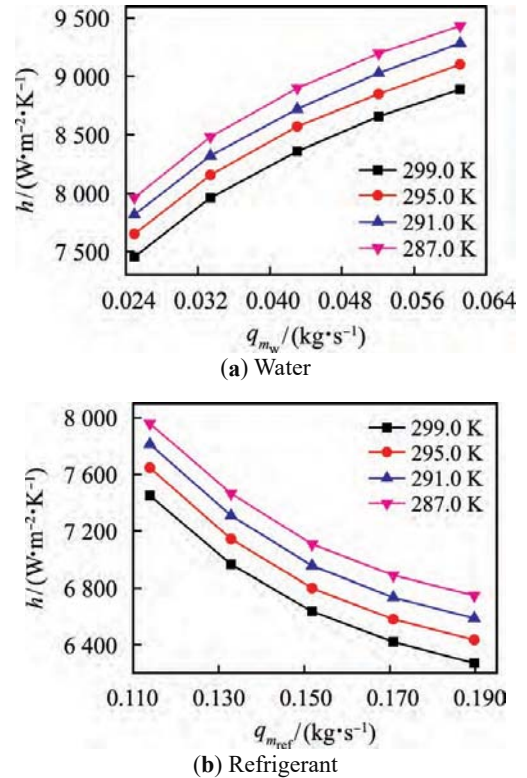
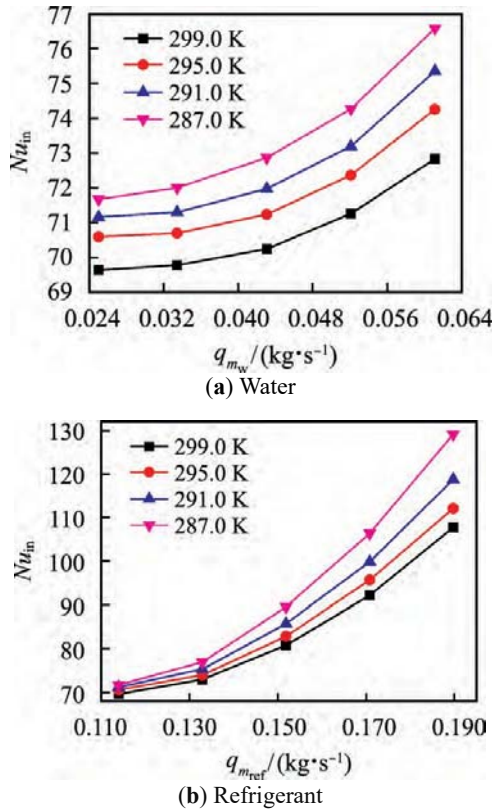


Figure 3. Variation of overall heat transfer coefficient with flow rate at the different inlet water temperature.

The variation of the inner tube Nusselt number ( $Nu_{\text{in}}$ ) with flow rate at the different inlet water temperature is given in Figures 4(a) and (b). It can be found that  $Nu_{\text{in}}$  increases with the increase of refrigerant flow rate and water flow rate ( $q_{m_{\text{ref}}}$  and  $q_{m_w}$ ) with the increase of 80.00% and 6.87%

respectively, which is due to the fact that the increase of flow rate can reduce the thermal boundary layer and make the heat transfer coefficient increase, which in turn shows  $Nu_{in}$  increase. Comparing the variation of  $Nu_{in}$  with the flow rate at different temperatures, it can be further found that the lower the inlet water temperature, the higher the inner pipe  $Nu_{in}$  is relatively at any flow rate, with a maximum increase of 19.85%. This is due to the increase in heat transfer rate caused by the increase in temperature difference by lowering the inlet water temperature, which leads to an increase in the heat transfer coefficient, resulting in a higher Nusselt number.



**Figure 4.** Variation of  $Nu_{in}$  with flow rate at the different inlet water temperature.

The variation of Nusselt number with flow rate for the outer tube at different inlet water temperatures is given in **Figures 5(a) and (b)**. **Figure 5(a)** indicates that  $Nu_{out}$  increases by 29.29% with the increase of  $q_{m_w}$ , for the higher the water flow, the more significant the increase of overall heat exchange. Although temperature difference caused by inner tube surface temperature and relatively low flow temperature increases,  $Nu_{out}$  still increase with the increase of  $q_{m_w}$ , lowering the inlet water

temperature, Nusselt number can be increased by 18.75%. **Figure 5(b)** gives the variation pattern of  $Nu_{in}$  with the increase of  $q_{m_{ref}}$  at different inlet water temperatures. It can be seen that  $Nu_{in}$  decreases by 11.17% with the increase of  $q_{m_{ref}}$ , which is attributed to the increase of the inner tube surface temperature due to the increase of  $q_{m_{ref}}$ . Since the temperature increases much faster than the heat transfer,  $Nu_{out}$  decreases with the increase of  $q_{m_{ref}}$ . At the lower inlet water temperature, the inner tube surface temperature is lower, causing  $Nu_{out}$  to increase by 2.21%.

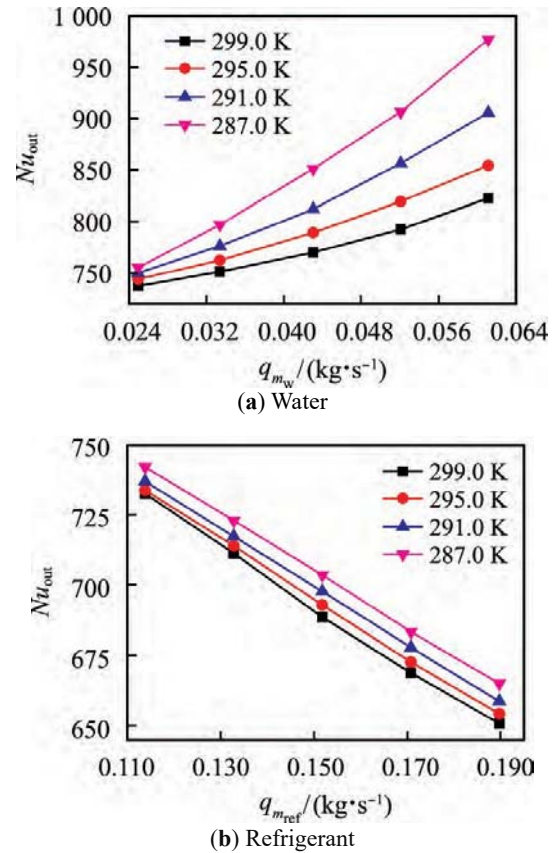


**Figure 5.** Variation of  $Nu_{out}$  with flowrate at the different inlet water temperature.

### 3.2 Effect of inlet refrigerant temperature on flow and heat transfer performance

The variation of the overall heat transfer coefficient with flow rate at the different inlet refrigerant temperatures is given in **Figures 6(a) and (b)**. As can be seen from **Figure 6**, the overall heat transfer coefficient increases by 18.80% with the increase in water flow rate, which is due to the increase in heat transfer rate and decrease in the average temperature difference due to the increase in chilled water flow rate. Under the condition of con-

stant water flow rate, increasing the flow rate of the inner tube refrigerant will lead to an increase in temperature difference, resulting in an overall heat transfer coefficient decrease of 15.84% with the increase in flow rate, again due to the higher flow rate of the inner tube refrigerant compared to the water flow rate and higher temperature, increasing the refrigerant flow rate, the overall heat transfer increase is relatively small, but the temperature difference between the import and export increases significantly, making the overall heat transfer coefficient decrease. It was also found that the overall heat transfer coefficient increased by 13.20% with the increase in inlet refrigerant temperature, which was due to the increase in the inlet refrigerant temperature, increasing the overall heat transfer coefficient despite the increase in temperature difference.

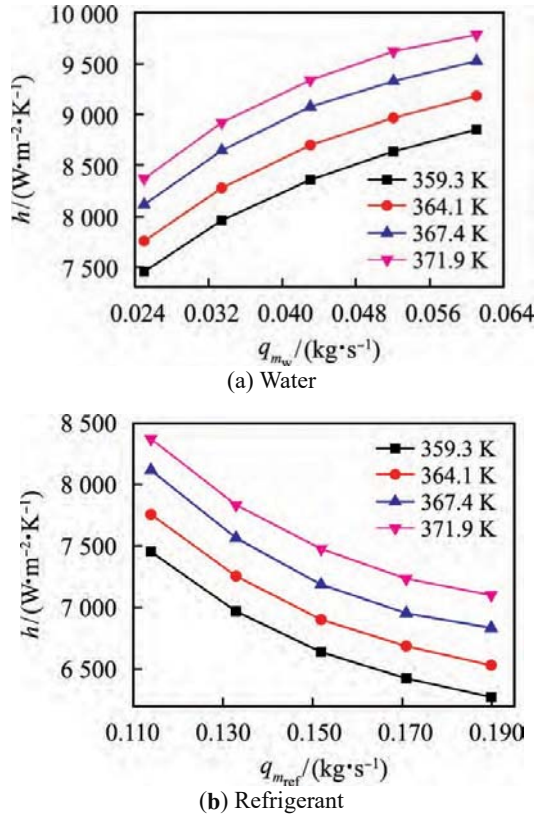


**Figure 6.** Variation of overall heat transfer coefficient with flow rate at the different inlet refrigerant temperature.

**Figures 7(a) and (b)** gives the variation of Nusselt number of the inner tube at different inlet refrigerant temperatures. It can be seen that  $Nu_{in}$  increases by 77.69% and 7.65% with the increase of flow rates of  $q_{m_{ref}}$  and  $q_{m_w}$ , which is more pronounced with the increase of refrigerant flow rates, due to the higher refrigerant flow rates compared to

water flow rates, which makes  $Nu_{in}$  increase significantly. The results also show that the higher the inlet refrigerant temperature, the higher the inner tube  $Nu_{in}$  relative to the water flow rate at any flow rate. This is due to the increase in the inlet refrigerant temperature, the increase in the heat transfer rate due to the increase in the temperature difference, leading to an increase in the overall heat transfer coefficient, resulting in a higher Nusselt number.

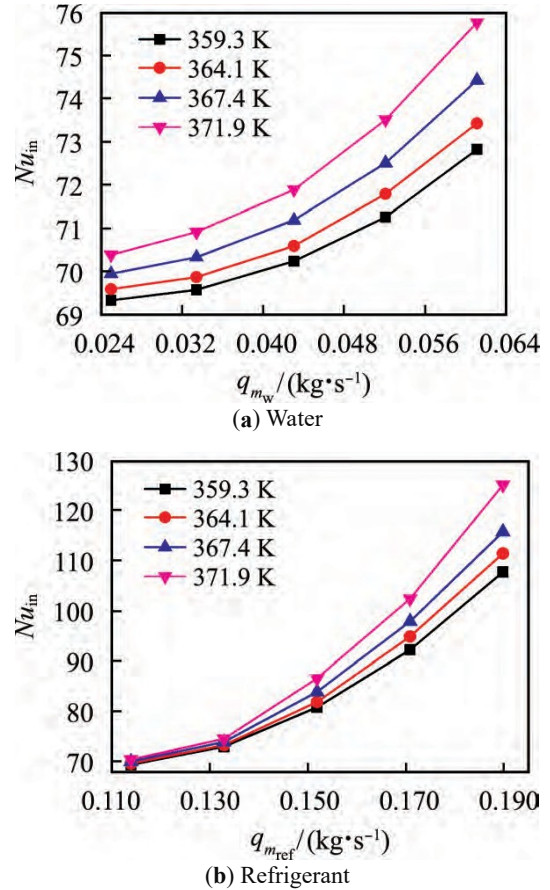


**Figure 7.** Variation of  $Nu_{in}$  with flow rate at the different inlet refrigerant temperature.

**Figures 8(a) and (b)** gives the variation of Nusselt number of the outer tube at different inlet refrigerant temperatures. From **Figure 8(a)**, it can be seen that  $Nu_{out}$  increases by 22.58% with the increase of  $q_{w_m}$ , which is due to the increase of the total overall heat transfer coefficient caused by the enhancement of turbulence with the higher water flow rate, showing that  $Nu_{out}$  increases with the increase of  $q_{w_m}$ . The higher the total heat transfer, the greater the overall heat transfer, and the Nusselt number increase by 10.61%. **Figure 8(b)** gives the variation pattern of  $Nu_{out}$  with  $q_{w_m}$ . It can be seen

that  $Nu_{out}$  decreases with the increase of  $q_{wm}$ , which is attributed to the increase of the temperature difference between the refrigerant temperature and the inner tube surface temperature due to the increase of  $q_{m_{ref}}$ , although the heat transfer increases,  $Nu_{out}$  still decreases with the increase of  $q_{m_{ref}}$ . Increasing the inlet refrigerant temperature,  $Nu_{out}$  value increases by 2.21% at the same flow rate.

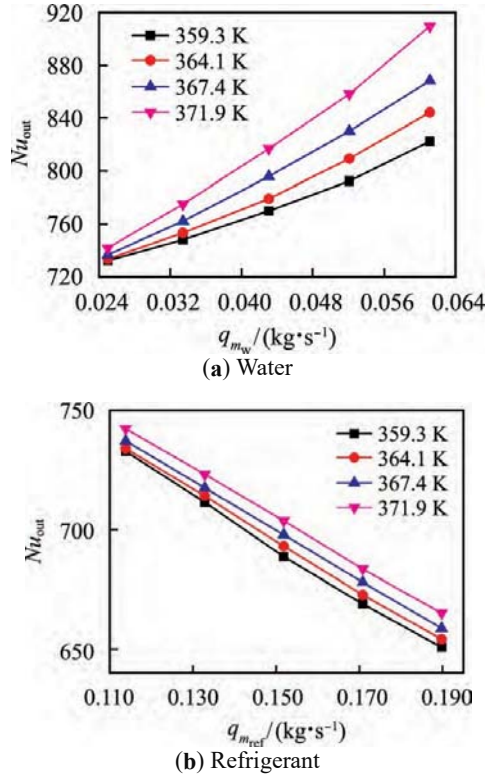


**Figure 8.** Variation of  $Nu_{out}$  with flow rate at the different inlet refrigerant temperature.

## 4. Conclusion

In this paper, the influence of fluid inlet flow parameters on the flow heat transfer characteristics of a multi-tube double-stage spiral casing heat exchanger was numerically analyzed, the influence law of the flow rate and temperature of the inner tube refrigerant and the flow rate and temperature of the outer tube water on the overall heat transfer performance of the heat exchanger and the Nusselt number of the inner and outer tubes was investigated, and conclusions were obtained.

(1) The overall heat transfer coefficient of the heat exchanger increases by 19.27% with the increase in water flow, but decreases by 15.84% with the increase in refrigerant flow, lowering the inlet

water temperature or increasing the refrigerant inlet temperature can increase the overall heat transfer coefficient by 6.82% and 13.20%, respectively.

(2)  $Nu_{in}$  increases by 7.65% and 80.00% with the increase of water and refrigerant flow rates,  $Nu_{out}$  increases by 29.29% with the increase of water flow rate but decreases by 11.17% with the increase of refrigerant flow rate,  $Nu_{in}$  and  $Nu_{out}$  all increase with the decrease of water temperature or increase of refrigerant temperature.

### Main symbols:

$A$	Heat exchange area, $m^2$
$d$	Pipe diameter, mm
$D$	Spiral diameter, mm
$h$	Overall heat transfer coefficient, $W/(m^2 \cdot K)$
$H$	Spiral pitch, mm
$K$	Thermal conductivity, $W/(m \cdot K)$
$L$	Spiral length, m
$q_m$	Mass flow rate, kg/s
$\Delta T$	Temperature difference, K
$\Phi$	Heat exchange, W

### Subscript:

Avg	Average value
In	Inner tube
Out	Outer tube
Ref	Refrigerant
w	Water

## Acknowledgements

This work is supported by the National Natural Science Foundation of China (51906265); the Science and Technology Innovation Talents Support Program of Henan Province (20HASTIT19); the Science and Technology Guidance Program of China Textile Industry Federation (2019073); the Key Scientific Research Support Project of Henan Province (21A470009); the Young Backbone Teacher Training Program of Zhongyuan University of Technology (2020XQG03).

## Conflict of interest

The authors declare that they have no interest of conflict.

## References

1. Omidi M, Farhadi M, Jafari M. A comprehensive review on double pipe heat exchangers. *Applied Thermal Engineering* 2017; 110: 1075–1090.
2. Omidi M, Farhadi M, Ali RDA. Numerical study of heat transfer on using lobed cross sections in helical coil heat exchangers: Effect of physical and geometrical parameters. *Energy Conversion and Management* 2018; 176: 236–245.

3. Dehghan B, Sisman A, Aydin M. Parametric investigation of helical ground heat exchangers for heat pump applications. *Energy and Buildings* 2016; 127: 999–1007.
4. Ren X, Wang Y, Peng J. The experimental system development of enhanced heat transfer in double pipe heat exchanger. *Refrigeration and Air Conditioning* 2014; 28(4): 469–471.
5. Liao B. Simulation research of impact of heat exchanger capacity of Heat exchanger casing's structural changes. *Refrigeration and Air Condition* 2010; 24(1): 40–44.
6. Zhang X, Xia X, Hao P. Experimental study on condensation heat transfer performance of R417a in spiral casing condenser. *Journal of Thermal Science and Technology* 2019; 18(2): 100–107.
7. Lv J, Ma Y, Cao K, *et al.* Design and experimental study on CO<sub>2</sub> water-cooled tube-intube gas cooler. *Journal of Refrigeration* 2016; 37(2): 113–118.
8. Ma R, Ma R, Wang Z, *et al.* Study on the new type tube-in-tube evaporative condenser performance. *Bulletin of Science and Technology* 2015; 31(7): 122–125.
9. Chen H, Gan X. Simulation and experiment study on performance of double-pipe heat exchanger. *Computer Simulation* 2015; 32(2): 256–260.
10. Colorado-Garrido D, Santogo-Castelazo E, Hernandez JA, *et al.* Heat transfer of a helical double pipe vertical evaporator: Theoretical analysis and experimental validation. *Applied Energy* 2009; 86(7-8): 1144–1153.
11. Wu Z, Wang L, Sundn B. Pressure drop and convective heat transfer of water and nanofluids in a double-pipe helical heat exchanger. *Applied Thermal Engineering* 2013; 60(1-2): 266–274.
12. Elattar HF, Fouda A, Nada SA, *et al.* Thermal and hydraulic numerical study for a novel multi tubes in tube helically coiled heat exchangers: Effects of operating/geometric parameters. *International Journal of Thermal Sciences* 2018; 128: 70–83.
13. Fouda A, Nada SA, Elattar HF, *et al.* Thermal performance modeling of turbulent flow in multi tube in tube helically coiled heat exchangers. *International Journal of Mechanical Sciences* 2018; 135: 621–638.
14. Liu X, Wang F, Li Z, *et al.* Parametric investigation of thermal-hydrodynamic performance in the innovative helically coiled heat exchangers in the heat pump system. *Energy and Buildings* 2020; 216: 109961.
15. Wang F, Fan X, Lian Z. Experimental study on an inverter heat pump with HFC125 operating near the refrigerant critical point. *Applied Thermal Engineering* 2012; 39: 1–7.
16. Wang F, Fan X, Lian Z, *et al.* Performance assessment of heat pumps using HFC125/HCs mixtures. *International Journal of Energy Research* 2011; 31: 135–147.
17. Sheeba A, Abhijith CM, Jose PM. Experimental and numerical investigations on the heat transfer and flow characteristics of a helical coil heat exchanger. *International Journal of Refrigeration* 2019; 99: 490–497.